The Plant Cell, Vol. 14, 2175–2190, September 2002, www.plantcell.org © 2002 American Society of Plant Biologists

The Regulation of Actin Organization by Actin-Depolymerizing Factor in Elongating Pollen Tubes[W]

Christine Y. Chen,[a,b] Eric I. Wong,[b] Luis Vidali,[c,1] Athena Estavillo,[b] Peter K. Hepler,[c,d] Hen-ming Wu,[a,b] and Alice Y. Cheung[a,b,d,2]

[a] Molecular and Cell Biology Program, University of Massachusetts, Amherst, Massachusetts 01003
[b] Department of Biochemistry and Molecular Biology, University of Massachusetts, Amherst, Massachusetts 01003
[c] Department of Biology, University of Massachusetts, Amherst, Massachusetts 01003
[d] Plant Biology Graduate Program, University of Massachusetts, Amherst, Massachusetts 01003

Pollen tube elongation is a polarized cell growth process that transports the male gametes from the stigma to the ovary for fertilization inside the ovules. Actomyosin-driven intracellular trafficking and active actin remodeling in the apical and subapical regions of pollen tubes are both important aspects of this rapid tip growth process. Actin-depolymerizing factor (ADF) and cofilin are actin binding proteins that enhance the depolymerization of microfilaments at their minus, or slow-growing, ends. A pollen-specific ADF from tobacco, NtADF1, was used to dissect the role of ADF in pollen tube growth. Overexpression of NtADF1 resulted in the reduction of fine, axially oriented actin cables in transformed pollen tubes and in the inhibition of pollen tube growth in a dose-dependent manner. Thus, the proper regulation of actin turnover by NtADF1 is critical for pollen tube growth. When expressed at a moderate level in pollen tubes elongating in in vitro cultures, green fluorescent protein (GFP)–tagged NtADF1 (GFP-NtADF1) associated predominantly with a subapical actin mesh composed of short actin filaments and with long actin cables in the shank. Similar labeling patterns were observed for GFP-NtADF1–expressing pollen tubes elongating within the pistil. A Ser-6-to-Asp conversion abolished the interaction between NtADF1 and F-actin in elongating pollen tubes and reduced its inhibitory effect on pollen tube growth significantly, suggesting that phosphorylation at Ser-6 may be a prominent regulatory mechanism for this pollen ADF. As with some ADF/cofilin, the in vitro actin-depolymerizing activity of recombinant NtADF1 was enhanced by slightly alkaline conditions. Because a pH gradient is known to exist in the apical region of elongating pollen tubes, it seems plausible that the in vivo actin-depolymerizing activity of NtADF1, and thus its contribution to actin dynamics, may be regulated spatially by differential H^+ concentrations in the apical region of elongating pollen tubes.

INTRODUCTION

Upon landing on the stigma, pollen grains hydrate and germinate, producing a polarized outgrowth, the pollen tube, which elongates over long distances to deliver the sperm cells to the embryo sacs within the ovules for fertilization (Lord, 2000; Palanivelu and Preuss, 2000; Cheung and Wu, 2001). Pollen tubes elongate by tip growth, whereby the pollen cytoplasm is restricted to the most proximal region of the extending tube by the periodic deposition of callose plugs some distance behind the apex. The actin cytoskeleton is known to play a key role in this rapid polarized cell growth process (Steer and Steer, 1989; Derksen et al., 1995; Hepler et al., 2001). Structurally, it is evident that filamentous actin is a prominent component of the pollen tubes.

In germinating pollen grains, actin filaments assemble around the germination pores just before tube emergence (Gibbon et al., 1999). Subsequently, many long actin cables are oriented axially throughout the shank of elongating pollen tubes. Secretory vesicles are transported by the actomyosin system to the apical region to deliver cell membrane and wall materials to support growth (Cheung et al., 2002). Depending on species and in individual tubes, the most proximal 5 to 50 μm of a pollen tube is dominated by what is known as the "clear zone," where the cytoplasm is occupied by densely packed secretory vesicles. Larger, more granular organelles are excluded from the clear zone.

[1] Current address: Brigham and Women's Hospital, Division of Hematology, LMR Center 301, 221 Longwood Avenue, Boston, MA 02115.
[2] To whom correspondence should be addressed. E-mail acheung@biochem.umass.edu; fax 413-545-3291.
[W] Online version contains Web-only data.
Article, publication date, and citation information can be found at www.plantcell.org/cgi/doi/10.1105/tpc.003038.

The streaming of secretory vesicles and other large organelles occurs in a reverse-fountain cytoplasmic streaming pattern in which the acropetal lanes move along the edge of the tube and then reverse direction at the base of the clear zone to move basipetally through the core of the tube. In elongating pollen tubes, long actin filaments usually do not enter the apical clear zone. Disorganized, short actin filaments have been observed in the subapical region and are most concentrated around the base of the clear zone. Recent studies using pharmaceutical and biochemical agents that interfere with actin polymerization indicate that cytoplasmic streaming can be uncoupled from growth, with tube elongation being substantially more sensitive to the inhibition of actin polymerization than cytoplasmic streaming (Vidali et al., 2001).

These and studies in other motile cell systems (Pollard et al., 2000; Pantaloni et al., 2001) have led to suggestions that the role of actin in pollen tube growth goes beyond the support of intracellular trafficking; instead, it appears that actin polymerization itself is linked intimately to the pollen tube elongation process. Spatially, the process of actin remodeling appears to occur at the base of the clear zone, where the cytoplasmic streams reverse directions (Hepler et al., 2001; Vidali and Hepler, 2001).

The factors that regulate the activity of pollen actin are far from being understood (Hepler et al., 2001). Multiple actin binding proteins regulate actin dynamics by maintaining the optimum equilibrium between unpolymerized actin molecules (G-actin) and assembled actin filaments (F-actin) required for the different cellular processes. Actin binding proteins that potentially affect the cytoskeleton architecture and dynamics, such as profilins, actin-depolymerizing factors (ADFs)/cofilins, villins, and fimbrims, all are present in pollen (McCurdy et al., 2001). ADF/cofilins are a large family of ubiquitous, low molecular mass (15 to 20 kD) actin binding proteins in eukaryotic cells. They are essential for many cellular processes and play critical roles in maintaining a cellular actin turnover rate significantly faster than the in vitro rates attained by purified actin filaments (Lappalainen and Drubin, 1997; Theriot, 1997; Carlier, 1998; Bamburg, 1999).

ADFs/cofilins bind to G- and F-actin and depolymerize F-actin primarily by preferentially enhancing the dissociation of actin monomers at the minus ends. Several ADFs/cofilins have been shown to sever actin filaments (Maciver et al., 1991; McGough et al., 1997; Maciver, 1998; McGough and Chiu, 1999). Mutations in ADFs/cofilins from different species have been associated with lethality, arrest in cell proliferation, and disorganized actin cytoskeletons. Their overexpression has resulted in increases of F-actin and actin bundles, enhanced cell movement, and membrane ruffling in *Dictyostelium discoideum* (Aizawa et al., 1996) and neurite outgrowth and extension in chicken and rat neurons (Meberg and Bamburg, 2000), but they also could induce lethality in yeast (Iida and Yahara, 1999).

In general, plant ADFs/cofilins have been referred to as ADFs (Staiger et al., 1997; Staiger, 2000). A maize ADF family, ZmADF1,2,3 (Lopez et al., 1996; Jiang et al., 1997b), and a nine-member ADF family from Arabidopsis, AtADFs (Carlier et al., 1997; Bowman et al., 2000; Dong et al., 2001a, 2001b), are the most thoroughly investigated plant ADFs. The deduced amino acid sequences of plant ADFs share ~40% similarity with vertebrate ADFs/cofilins. Overexpression and underexpression of AtADF1 in transformed Arabidopsis resulted in disruption of the normal actin cytoskeleton in several cell types and led to phenotypes that suggest its importance to cell expansion, organ growth, and flowering (Dong et al., 2001b). Furthermore, several green fluorescent protein (GFP)–AtADF fusion proteins, including GFP-AtADF1, have been observed to bind to actin filaments, and these AtADFs also affect F-actin organization in transiently transformed BY2 cells (Dong et al., 2001a).

In maize roots, immunolocalization of the vegetative cell–expressed ZmADF3 showed that it redistributed from a diffuse to a tip-concentrated location as root hairs emerged and elongated (Jiang et al., 1997a). This finding is similar to observations that ADFs/cofilins localize to the leading edge of other migrating cells, where active actin remodeling is expected to occur, suggesting a probable analogous role in tip-growing root hairs.

Similar to a number of other cytoskeletal components, pollen-specific ADFs apparently have diverged significantly from their vegetative or constitutively expressed counterparts (Lopez et al., 1996). ADFs are believed to play critical roles in regulating actin dynamics in pollen tubes because they are known to be regulated by factors such as protons, calcium, and phosphatidylinositol-4-monophosphate 2, which are important regulators of pollen tube growth (Franklin-Tong, 1999; Hepler et al., 2001).

Here, we report the characterization of a pollen-specific ADF, NtADF1, from tobacco. In elongating pollen tubes, GFP-NtADF1 associated predominantly with an actin mesh at the subapical region and with long cables along the shank of these tubes. Overexpression of NtADF1 in elongating pollen tubes resulted in the disruption of the actin cytoskeleton and reduced growth rates. Our results show that the Ser-6 residue in NtADF1 is critical for its interaction with actin. We also observed that the in vitro actin-depolymerizing activity of NtADF1 is favored by a slightly alkaline pH, a condition known to occur at the subapical region of elongating pollen tubes, where the ADF-rich actin mesh is located. Our results suggest that NtADF1 plays a critical role in regulating the proper balance of actin polymerization and depolymerization needed for an optimum pollen tube growth process.

RESULTS

Isolation and Characterization of Tobacco Pollen-Specific ADF cDNAs

We isolated several tobacco pollen cDNA clones using the Arabidopsis AtADF1 cDNA (Carlier et al., 1997) as a probe.

Of the eight completely characterized cDNAs, six belonged to one class (*NtADF1*) and two belonged to another class (*NtADF2*). The deduced amino acid sequences of NtADF1 and NtADF2 are shown in Figure 1A. Both isoforms are predicted to have 137 amino acid residues with a molecular mass of 15 kD. They are 88% identical and 95% similar to each other. The amino acid sequence alignment between NtADF1, NtADF2, the maize pollen-specific ZmADF1 and vegetative ZmADF3, Arabidopsis vegetative AtADF1, yeast cofilin-1, and human dextrin (Figure 1) shows between 60 and 70% identity and up to 85% similarity among the plant ADFs and ~40% identity and 60% similarity between NtADF1 and animal and yeast cofilin.

In particular, NtADF1 is 68% identical and 86% similar to the pollen ZmADF1, whereas these levels decrease to 58 and 79%, respectively, compared with the vegetatively expressed ZmADF3, consistent with the view that pollen-expressed genes are substantially more diverged from their vegetative counterparts (Huang et al., 1996; Meagher et al., 1999a, 1999b). The deduced secondary structure of NtADF1 also shows significant homology with other ADF/cofilins. Its predicted tertiary structure is highly similar to the determined structures of yeast cofilin (Federov et al., 1997) (Figure 1B), AtADF1 (Bowman et al., 2000) (data not shown), and actophorin (Leonard et al., 1997) (data not shown). It is interesting that the pI values of plant ADFs characterized to date are considerably more acidic (e.g., NtADF1 has a pI of ~5 and AtADF1 has a pI of ~6) compared with the pI values of animal ADFs, which range between 7 and 9 (e.g., human dextrin has a pI of ~9).

RNA gel blot analysis showed that *NtADF1* mRNA was present exclusively in pollen grains and tubes (Figure 1C). *NtADF2* mRNA also was exclusive to pollen, but its level was significantly lower (data not shown), as expected from the lower frequency with which it appeared in the cDNA library. A lack of cross-hybridization with nonpollen RNA suggests that NtADF1 is quite diverged from its counterparts expressed in vegetative or even female reproductive tissues. Initial analysis suggested that NtADF1 and NtADF2 behave similarly, so we focused our studies on NtADF1.

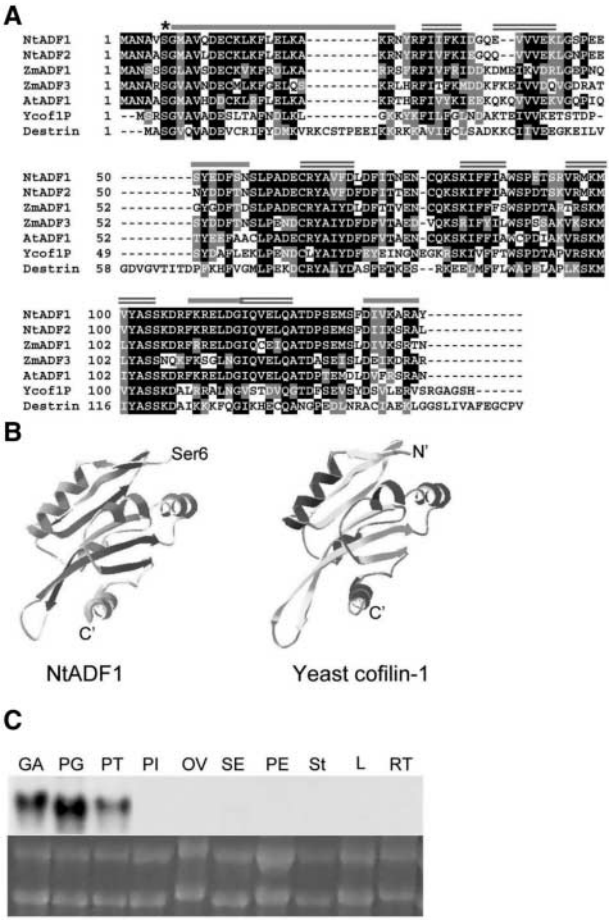

Figure 1. Structure and Expression of NtADF1.

(A) Deduced amino acid sequence alignment between NtADF1, NtADF2, Arabidopsis AtADF1, maize pollen ZmADF1, constitutive ZmADF3, yeast cofilin, and human dextrin. The asterisk indicates the Ser-6 residue that has been mutagenized to yield NtADF1(S6A) and NtADF1(S6D). Black shading indicates identity, gray shading indicates similarity, and dashes indicate gaps. Conserved predicted secondary structures (predicted by PREDATOR-EMBL) are shown by overlines: single lines indicate α-helices, and double lines indicate β-sheets.

(B) Predicted tertiary structure of NtADF1 (left) (produced by the Swiss-Model program and colored with the Swiss-PBD Viewer) and the determined tertiary structure of yeast cofilin (Federov et al., 1997) (right).

(C) RNA gel blot analysis of NtADF1. Comparable levels of total RNA (bottom) were loaded for RNA gel blot analysis. ^{32}P-labeled NtADF1 cDNA was used as a probe for hybridization (top). GA, green anther; PG, pollen grains; PT, pollen tubes; PI, pistil (stigma, style, and ovary); OV, ovary; SE, sepal; PE, petal; St, stigma and style; L, leaf; RT, root.

GFP-NtADF1 Associates with Dynamic Actin Cables in Elongating Pollen Tubes

Both N- and C-terminal GFP (Tsien, 1998) fusions with ADFs/cofilins have been used to visualize their interactions with the actin cytoskeleton (Aizawa et al., 1997; Bernstein et al., 2000; Dong et al., 2001a). In initial characterizations, N- or C-terminal GFP fusions with NtADF1 showed very similar labeling patterns in elongating pollen tubes, so we relied on the N-terminal fusion protein GFP-NtADF1 to examine the localization pattern of NtADF1 in pollen. The Lat52 promoter (Twell et al., 1990) was used to drive the pollen-specific expression of transgenes in these studies.

Expression from GFP-containing transgenes in transiently

transformed pollen tubes usually was detectable between 2 and 3 h after microprojectile bombardment transformation of pollen grains. A majority of germination-competent pollen usually developed a polar protrusion within 30 min after cultivation on in vitro medium. These transiently transformed pollen grains showed a range of GFP-NtADF1 labeling patterns that correlated with fluorescence intensity. Pollen grains that showed the highest levels of green fluorescence usually had a GFP-NtADF1 labeling pattern associated with thick bundles and patches (Figure 2A, right). These pollen grains usually failed to germinate. If pollen tubes developed from this class of pollen grains, growth was aborted soon after germination.

Pollen grains with low but clearly observable levels of green fluorescence usually showed GFP-NtADF1 association with thin cables that could be long and spiraling (Figure 2A, left). These pollen grains usually were competent to germinate. Pollen tubes that developed from this class of grains elongated relatively normally for at least 6 to 8 h after germination (see below) and showed detectable levels of GFP-NtADF1 (Figure 2B). GFP-NtADF1 distributed throughout the pollen tube cytosol but was observed readily to associate with dynamic filamentous structures in the shank (Figure 2B). These thin cables in the pollen tube shank aligned mostly with the long axis of the tubes. However, GFP-NtADF1 appeared to converge around the base of the clear zone and associated prominently with a mesh of relatively short, disorganized, but highly active cables and filaments in this subapical region (Figure 2B, arrow).

In the shank, the GFP-NtADF1–labeled cables along the cortical region moved toward the tip and those closer to the center of the tube moved toward the grain (see supplemental data online), typical of the reverse-fountain cytoplasmic streaming pattern. The GFP-NtADF1–labeled mesh at the subapical region was located near where the GFP-NtADF1–labeled cables and cytoplasmic streams reversed directions. The relatively long GFP-NtADF1–labeled cables were not observed to invade the clear zone, although short and

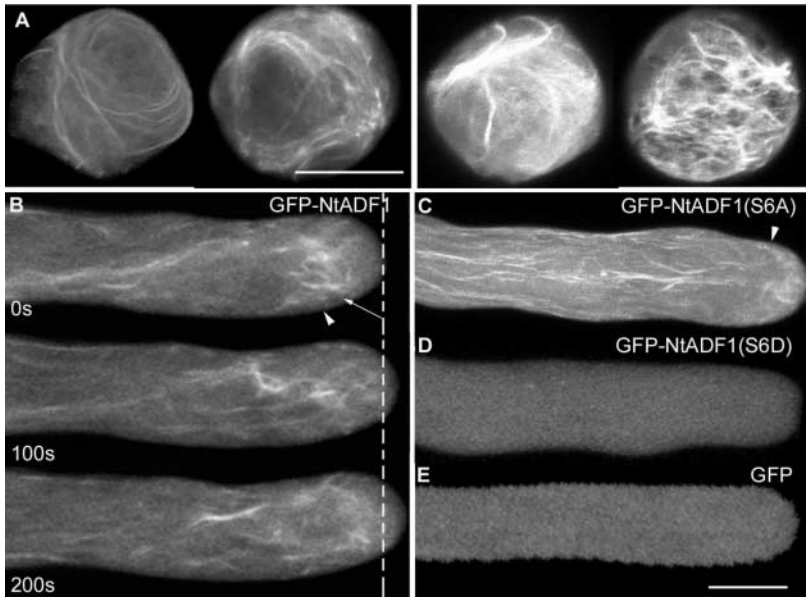

Figure 2. GFP-NtADF1 Associates with Dynamic Actin Bundles in Elongating Pollen Tubes.

(A) GFP-NtADF1 labeling pattern in two pollen grains representative of those expressing a moderate level of green fluorescence (left). Two pollen grains representative of those with high levels of GFP-NtADF1 expression are shown (right). Micrographs shown are projections of 1-μm optical sections through the entire grains. Bar = 20 μm.

(B) GFP-NtADF1 labeling pattern in an elongating pollen tube representative of those that expressed a moderate level of this fusion protein. Confocal laser scanning images of the same optical section were obtained over a period of 200 s. Time interval is indicated at bottom left in each image. The dotted line indicates the tube tip location at the beginning of the time series. Arrowheads indicate the base of the clear zone, where cytoplasmic streams reversed direction (as observed by differential interference contrast imaging). Arrow indicates the subapical actin mesh. Phalloidin staining of similarly transformed pollen tubes confirmed that the GFP-NtADF1–labeled structures were actin cables (see Figure 3). The streaming pattern of these GFP-NtADF1–labeled cables can be seen in the supplemental data online.

(C) Single optical section of a representative GFP-NtADF1(S6A)–expressing pollen tube.

(D) Single optical section of a GFP-NtADF1(S6D)–expressing pollen tube.

(E) Single optical section of a GFP-expressing pollen tube.

Pollen grains and tubes were transformed transiently by microprojectile bombardment. Bar = 10 μm.

significantly finer filaments could be seen within the clear zone and moving basipetally (see supplemental data online).

Cytosolic green fluorescence in the transiently transformed pollen tubes most likely reflect free GFP-NtADF1 and those that have bound to G actin, which is known to be abundant in pollen tubes (Vidali and Hepler, 1997; Gibbon et al., 1999), and recombinant NtADF1 has been observed to bind to G-actin in vitro (data not shown). The GFP-NtADF1–labeled cables were very similar to actin structures revealed by fluorescently labeled phalloidin staining of chemically fixed pollen tubes (Geitmann et al., 2000; Vidali et al., 2001) (Figure 3). They also mimic structures revealed by GFP-talin labeling (F-actin binding domain of mouse talin) in transformed elongating pollen tubes (Kost et al., 1999; Fu et al., 2001).

When transformed pollen tubes expressing GFP-NtADF1 were observed after chemical fixation and staining with fluorescently labeled phalloidin, the GFP-NtADF1–labeled structures coincided with phalloidin-labeled cables (Figure 3, top row), indicating that GFP-NtADF1 associated with actin filaments. Binding of GFP-NtADF1 to actin cables in elongating pollen tubes was consistent with the ability of recombinant NtADF1 to cosediment with F-actin efficiently in vitro (Figure 4A). GFP-AtADFs also have been reported to bind to actin cables in vegetative cells (Dong et al., 2001a).

GFP-NtADF1 Associates with an Actin Mesh in the Subapical Region of Pollen Tubes

At the lowest detectable level of transgene expression, GFP-NtADF1 associated most prominently with a mesh of short filaments at the subapical tube region (Figure 5). Fine actin filamentous structures (Kost et al., 1999) and short actin bundles (Fu et al., 2001) have been reported previously in GFP-talin–expressing transformed tobacco pollen tubes. We also observed a GFP-talin–labeled mesh in transformed tobacco pollen tubes (data not shown). Phalloidin labeling of fixed pollen tubes from several species also revealed a concentrated network of actin cables at a similar subapical region (Derksen et al., 1995; Gibbon et al., 1999; Geitmann et al., 2000; Vidali et al., 2001). These findings left little doubt that the GFP-NtADF1–labeled structure at the subapical region of elongating tobacco pollen tubes was composed of a dense, ADF-rich network of highly dynamic short actin cables and filaments.

In individual pollen tubes, the GFP-NtADF1–labeled actin mesh was located between 1 and 5 μm from the tube apex. They were invariably slightly proximal to the base of the clear zone, which, in tobacco, is located $\sim$2 to 5 μm from the pollen tube tip (Figure 5A) and could be discerned by differential interference contrast imaging. That this ADF-rich actin mesh could be critical for growth was suggested by the absence of the GFP-NtADF1–labeled structure in growth-arrested pollen tubes (data not shown). Furthermore, the orientation of this actin mesh was always maintained approximately perpendicular to the growth axis, even when a pollen tube was reorienting its growth trajectory (Figure 5A and supplemental data online), implying a relationship of this structure to growth orientation.

GFP–Lily ADF Associates with an Actin Mesh in the Alkaline Band Region of Elongating Lily Pollen Tubes

Actin remodeling at the subapical region of elongating pollen tubes, where cytoplasmic streams reverse directions at the base of the clear zone, has been suggested to be important for pollen tube growth (Hepler et al., 2001). That the actin-depolymerizing activity of ADFs could play a critical role in maintaining the level of actin dynamics necessary for pollen tube elongation seems plausible. ADFs/cofilins from many species are known to depolymerize actin more efficiently under alkaline conditions (pH 7.7 to 8.5) (Hawkins et al., 1993; Gungabissoon et al., 1998; Maciver et al., 1998; Bernstein et al., 2000). Thus, their actin-depolymerizing ability could be regulated by subtle differences in H^+ concentration within the cell, both spatially and temporally.

We have observed that recombinant NtADF1 depolymerized F-actin in vitro more efficiently at pH 8.0 than at pH 6.0 (Figure 4B). This finding suggests that the actin-interacting activity of NtADF1 may be modulated along a pH gradient, such as that generated by differential proton fluxes at the tip and subapical regions of elongating pollen tubes (Feijo et al., 1999) (Figure 5E). To correlate the location of the ADF-rich actin mesh to intracellular H^+ conditions, we used lily pollen tubes, in which a tip-concentrated H^+ gradient and a subapical alkaline band in the proximity of the base of the clear zone have been observed (Feijo et al., 1999).

A lily anther–expressed ADF clone has been described previously (LlADF) (Kim et al., 1993). GFP-LlADF fusion protein was expressed transiently by the maize pollen-specific pZmc13 promoter (Hamilton et al., 1998) in bombarded lily pollen tubes. A GFP-LlADF–labeled dynamic structure similar to that observed in tobacco pollen tubes was observed in the subapical region of these transformed lily pollen tubes (Figure 5B and supplemental data online). Projection of optical sections across the entire tube revealed a GFP-LlADF–labeled band at the subapical region that was also trailed by a funnel-shaped green fluorescent structure similar to that reported in phalloidin-stained chemically fixed lily pollen tubes (Vidali et al., 2001). This GFP-LlADF–labeled actin mesh usually was 10 to 15 μm from the tube apex, which also was approximately halfway between the tip and the base of the clear zone.

The exact spatial relationship between the ADF-rich actin mesh and intracellular H^+ conditions remains to be determined. However, it is apparent that GFP-LlADF was prominently associated with actin filaments in a region relatively more alkaline than the apex (Feijo et al., 1999). A similar spatial relationship between the GFP-NtADF1–labeled actin mesh and intracellular H^+ concentration likely

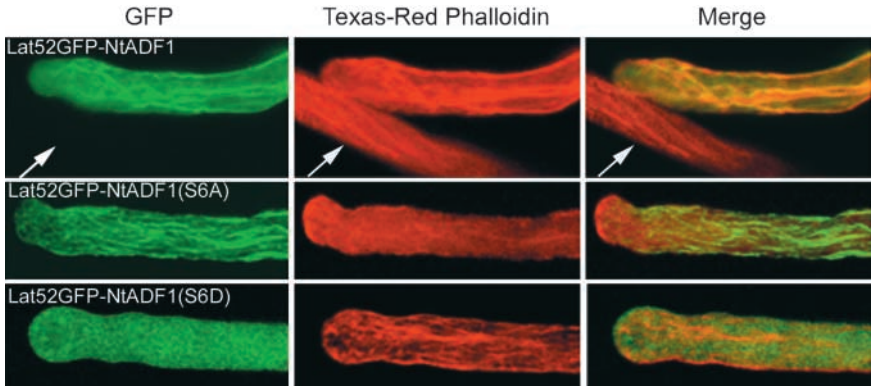

Figure 3. GFP-NtADF1 Associates with Actin Filaments in Elongating Transformed Pollen Tubes, and Ser-6 Is Important for This Binding.

Projections of a Z-series of 1-μm optical sections through entire chemically fixed pollen tubes that expressed GFP-NtADF1 (top row), GFP-NtADF1(S6A) (middle row), or GFP-NtADF1(S6D) (bottom row). These pollen tubes, which were transformed transiently by microprojectile bombardment, elongated normally at the time of chemical fixation, which was followed by Texas red–conjugated phalloidin staining (Doris and Steer, 1996; Vidali et al., 2001). The same pollen tubes are shown in each row. The left column shows GFP fluorescence, the middle column shows red fluorescence from phalloidin binding, and the right column shows a merged image of green and red fluorescence of the same tube. Orange/yellow color indicates colocalization of GFP-NtADF1 and phalloidin. Arrows point to a nontransformed pollen tube showing only red fluorescence from phalloidin binding but no green fluorescence. Note that in the GFP-NtADF1(S6A)–expressing tube, phalloidin binding (middle) was almost entirely excluded.

exists in tobacco pollen tubes in which differential H^+ fluxes around the tube tip have been observed (C. Chen, H. Wu, A.Y. Cheung, and J. Kunbel, unpublished data).

Ser-6 in NtADF1 Is Important for Interaction with Actin

Amino acid sequence and structural conservation around the Ser-6 residue in NtADF1 with Ser-3 of mammalian and Ser-6 of other plant ADFs/cofilins (Figures 1A and 1B) suggest functional analogy. Phosphorylation or mutation of this N-terminally located Ser residue to an acidic amino acid in several ADFs/cofilins resulted in the abolition of their actin binding activity (Agnew et al., 1995; Moriyama et al., 1996; Smertenko et al., 1998; Bamburg et al., 1999), implying an important role for this Ser residue in regulating the activity of these actin binding proteins. However, phosphorylation at this N-terminally located Ser residue is not a universal mechanism to regulate ADF/cofilin activity, because yeast and *Dictyostelium* cofilins have not been observed to be phosphorylated (Lappalainen et al., 1997; Bamburg et al., 1999).

To determine whether Ser-6 in NtADF1 plays a similar role, an Ala (S6A) or an Asp (S6D) substitution was introduced into NtADF1. When GFP fusions of either of these mutant proteins were expressed at moderate levels where green fluorescence was clearly detectable but not excessive, pollen tubes elongated relatively normally for at least 6 to 8 h after germination (see below). GFP-NtADF1(S6A) showed similar but enhanced association with actin cables as GFP-NtADF1, except that a relatively strong association with cortical actin cables was observed as well (Figure 2C). On the other hand, GFP-NtADF1(S6D) was exclusively cytosolic (Figure 2D), as in control pollen tubes that expressed GFP alone (Figure 2E).

In chemically fixed pollen tubes, GFP-NtADF1(S6A) showed intense labeling of actin cables, whereas phalloidin binding was precluded almost entirely (Figure 3, middle row), suggesting very strong binding of GFP-NtADF1(S6A) to actin filaments and consistent with previous reports that ADF/cofilin binding to actin filaments altered their conformation and diminished phalloidin binding (Hayden et al., 1993). In contrast, pollen tubes expressing GFP-NtADF1(S6D) showed predominantly diffuse fluorescence in the cytosol, whereas phalloidin binding clearly revealed the presence of actin cables in these tubes (Figure 3, bottom row). These observations and previous literature on animal ADF/cofilin indicate that the in vivo actin binding activity of NtADF1 is dependent on the phosphorylation state at the hydroxyl side chain of Ser-6. In vitro, recombinant NtADF1(S6D) also did not cosediment with F-actin as efficiently as its wild-type or S6A counterparts (Figure 4A).

Disruption of the Pollen ADF Condition Suppresses Elongation Rates and Disturbs the Actin Cytoskeleton in Transiently Transformed Pollen Tubes

Inhibition of actin polymerization by chemical or biochemical agents has a profound effect on pollen tube growth, leading

to the disorganization of actin and growth arrest (Gibbon et al., 1999; Vidali et al., 2001). To examine how pollen tubes react to altered ADF levels or activities, Lat52-driven NtADF1, its S6A mutant transgene, and its S6D mutant transgene were coexpressed transiently with Lat52-GFP in microprojectile-bombarded pollen. GFP expression would act as an indicator of cotransformed pollen tubes. We established previously that the level of transgene expression correlates linearly with the amount of input DNA (Chen, 2002). Figure 6A shows that increasing amounts of Lat52-NtADF1 transgene introduced into these pollen tubes was associated with increasingly reduced pollen tube growth rates.

The effect of NtADF1(S6A) was more severe than that of NtADF1, whereas NtADF1(S6D) had little effect on pollen tube growth (Figure 6B). Overexpression of GFP-tagged NtADF1 and NtADF1(S6A) was less adverse to pollen tube growth than overexpression of their untagged counterparts (Figure 6A). This was consistent with observations that most of the pollen tubes that expressed moderate levels of GFP-NtADF1 or GFP-NtADF1(S6A) showed relatively normal growth properties (Figures 2, 3, and 5), allowing them to be good markers for ADF localization and dynamics.

When the cytoskeleton in the growth-inhibited pollen tubes was examined (Figure 6C), the number of fine, long axially aligned actin cables seen in control elongating tubes was reduced significantly in NtADF1-overexpressing tubes, and the subapical concentration of actin also was abolished. Overexpression of NtADF1 also induced substantial aggregation of actin, because thick actin bundles often were seen in these tubes. The actin cytoskeleton in pollen tubes that overexpressed NtADF1(S6D) remained similar to that in control tubes (data not shown), consistent with the inability of this mutant protein to interact appreciably with actin.

GFP-NtADF1 Localization Pattern in Pollen Tubes Elongating in the Pistil

We obtained a large number of transgenic tobacco plants that were transformed by the pollen-expressed Lat52-GFP-NtADF1 wild-type, S6A, or S6D transgenes. When germinated in in vitro medium, pollen from plants expressing GFP-NtADF1 or GFP-NtADF1(S6A) consistently showed lower levels of fluorescence relative to that observed in transiently transformed tubes. This finding suggests strong endogenous mechanisms, either during pollen development or at maturation, to regulate the level of ADFs to prevent levels that would have been deleterious to pollen germination and tube growth.

When germinated in vitro, the stable transformed GFP-NtADF1– and GFP-NtADF1(S6A)–expressing pollen tubes showed similar green fluorescence labeling patterns as those observed in transiently transformed pollen tubes that expressed these fusion proteins, including the actin mesh at the subapical region (Figures 2 and 5), although the cytosolic signal usually was higher. GFP-NtADF1(S6D) was localized exclusively in the cytosol (data not shown). The in vitro growth characteristics of these transformed pollen tubes appeared relatively normal, as was their reproductive yield by self-pollination, suggesting that their in vivo elongation capacity was not impaired.

Pollen from Lat52-GFP-NtADF1–transformed plants provided an opportunity to observe the GFP-NtADF1–labeled actin cytoskeleton structure in pollen tubes elongating within the pistil. GFP-NtADF1 in these stable transformed pollen grains was associated with spiraling actin cables (Figure 7C), similar to those observed in transiently transformed grains (Figure 2A, left). In styles pollinated by pollen expressing GFP-NtADF1, we observed that a majority of GFP-NtADF1–expressing tubes had reached the lower half of the style, similar to control GFP-expressing tubes and consistent with a comparable reproductive yield in these plants after self-pollination.

Most of these GFP-NtADF1–expressing tubes showed strong green fluorescence at the subapical region, along with a diffuse green fluorescent signal throughout the cytosol and occasional actin cables (Figure 7E). Although not as discrete, the subapical concentration of GFP-NtADF1 mimicked that observed in transiently transformed and in vitro–grown pollen tubes (Figures 2 and 5).

When the stigmatic regions of pistils pollinated by GFP-NtADF1–expressing or control GFP-expressing pollen were examined, a considerably larger number of GFP-NtADF1–expressing tubes was observed to have remained within the stigmatic region, whereas only a few GFP-expressing grains remained there in control stigmas (Figures 7A and 7B). Contrary to the more diffuse GFP-NtADF1–labeling pattern observed in more elongated pollen tubes in the style (Figure 7E), many of these shorter GFP-NtADF1–expressing tubes in the stigmatic region showed an abundance of GFP-NtADF1–labeled actin cables throughout the tube (Figure 7D). These shorter GFP-NtADF1–expressing pollen tubes also generally showed a higher level of green fluorescence than those extended into the styles, suggesting that quantitative differences in expression from the Lat52-GFP-NtADF1 transgene between pollen grains could have retarded the growth of some of these tubes.

DISCUSSION

During pollen tube growth, a rapid rate of actin turnover must keep pace with the equally rapid rates of tube elongation. The results from this study indicate that ADF may play a crucial role in the regulation of actin remodeling in this tip growth process. Overexpression studies involving NtADF1 indicate that the rate of pollen tube growth is fine-tuned to the level of ADF, with increasing amounts of the actin binding protein progressively causing an inhibition of growth. GFP-NtADF1 colocalizes with filamentous actin in pollen,

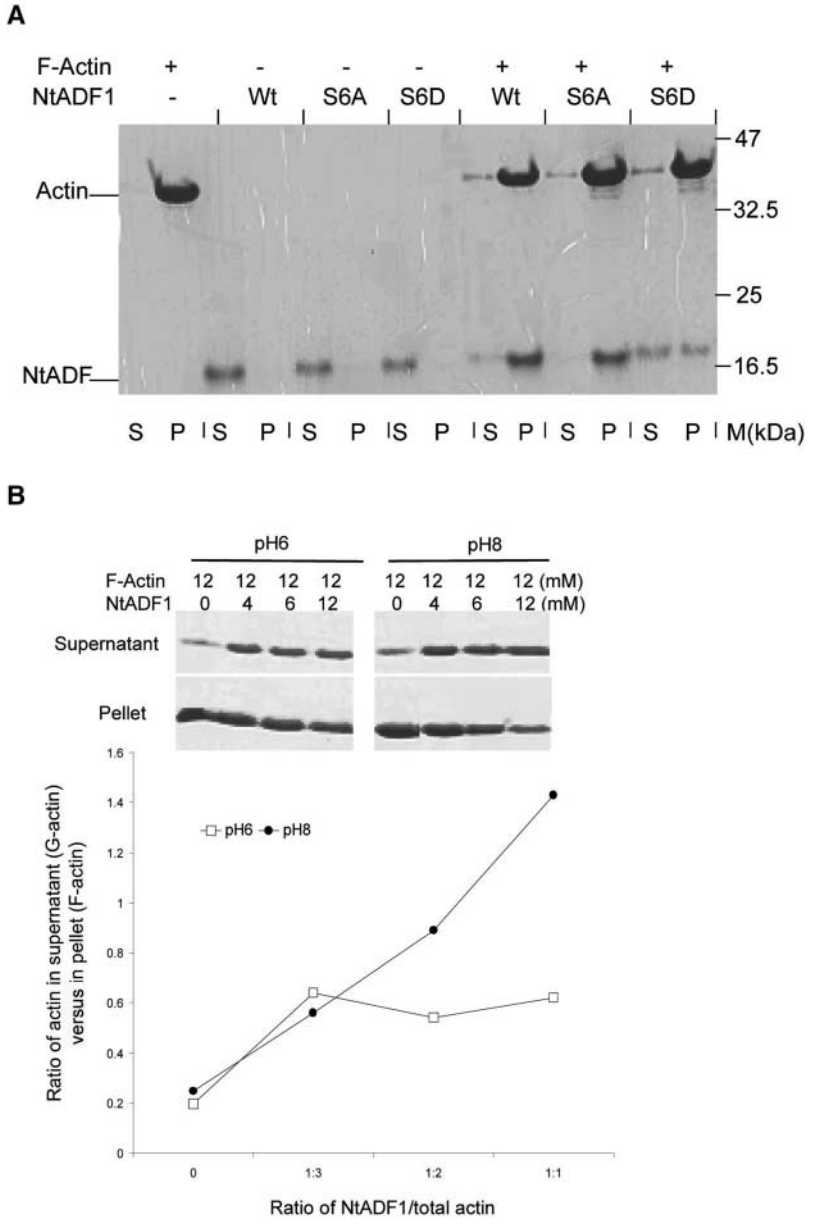

Figure 4. NtADF1 Cosediments with F-Actin.

(A) F-actin was mixed with recombinant NtADF1 (Wt), NtADF1(S6A), or NtADF1(S6D) as indicated. After cosedimentation by ultracentrifugation, the pelleted proteins were resuspended in a volume of SDS-PAGE loading buffer equal to that of the supernatant. Equal volumes of these pelleted proteins and proteins in the supernatant were analyzed by 15% SDS-PAGE. This was followed by Coomassie blue staining. M, molecular mass marker; P, pellet; S, supernatant.

(B) In vitro NtADF1–depolymerizing activity on F-actin. F-actin and NtADF1 was mixed in the ratios indicated. F- and G-actin were separated by ultracentrifugation. The pelleted proteins and supernatant proteins were treated as described above. The ratio of actin in the supernatant (G-actin) to that in the pellet (F-actin) was determined by densitometry scanning. The gels at top show SDS-PAGE results demonstrating the level of G- and F-actin under different actin/NtADF1 ratios and at two different pH values, 6 and 8. The graph at bottom shows the ratios of G- to F-actin under different NtADF1/actin ratios plotted from this representative experiment. Closed circles, pH 8; open squares, pH 6.

especially at the base of the clear zone. Previous imaging studies have shown that the base of the clear zone, where remodeling is thought to occur, is characterized by the presence of an alkaline band (Feijo et al., 1999); the in vitro studies reported here show that the actin binding activity of NtADF1 is enhanced by alkaline pH. Together, these observations provide compelling support for a role for pollen ADF in the control of actin dynamics in growing pollen tubes.

Ser-6 in NtADF1 Regulates Its Actin-Interacting Activity in Vivo and in Vitro

We have shown by in vitro F-actin cosedimentation assays (Figure 4A) and in vivo localization of GFP-NtADF1 in elongating pollen tubes (Figure 3) that the charge characteristic at Ser-6 was important for the interaction between NtADF1 and F-actin. Although the in vitro interaction was not enhanced substantially by the S6A substitution (Figure 4A), its effect in vivo was more pronounced, as revealed by the substantially stronger GFP-NtADF1(S6A) binding to actin cables in elongating pollen tubes relative to GFP-NtADF1 (Figures 2B, 2C, and 3). On the other hand, although the effect of the S6D substitution was detectable in vitro (Figure 4A), it was relatively mild compared with the apparent failure of GFP-NtADF1(S6D) to associate with actin filaments in vivo (Figures 2D and 3).

The phosphorylation at Ser-3 of animal ADFs/cofilins is known to be a major regulatory mechanism for their activity (Moriyama et al., 1996; Bamburg, 1999). In plants, in vitro phosphorylation of ZmADF3 at the analogous Ser-6 position abolishes the actin binding activity of these proteins (Smertenko et al., 1998), and when overexpressed, Arabidopsis AtADF1 has been observed to exist in phosphorylated and nonphosphorylated forms (Dong et al., 2001b). Therefore, our data are consistent with phosphorylation at the Ser-6 position of NtADF1 being an important regulatory mechanism for its activity in elongating pollen tubes.

NtADF1 and Actin Interaction in Live Elongating Pollen Tubes

When expressed at moderate levels, GFP-NtADF1 associates with long, axially arranged actin cables and short disorganized actin filaments in the shank and at the subapical region of elongating pollen tubes (Figures 2, 3, and 5). Immunolocalization studies of pollen ADFs have been performed only in chemically fixed daffodil pollen grains and tubes using antibodies against the maize pollen ZmADF3 (Smertenko et al., 2001). Daffodil ADFs have been observed to associate with actin arrays and rodlets in pollen grains. Except for a few granules, ADFs did not associate with any specific structural features in chemically fixed daffodil pollen tubes; instead, they appeared diffuse throughout the cytosol.

These observations are in contrast to those presented here showing a distinct association between GFP-NtADF1 and F-actin (Figures 2, 3, and 5). ADF and actin were colocalized at the tip of chemically fixed daffodil pollen tubes that had adhered to the growth surface. It is not possible to determine whether these structures were analogous to the GFP-NtADF1–labeled actin mesh at the subapical region of elongating tubes shown here (Figures 2 and 5). However, the labeling of actin cables in live cells has been reported for several GFP-AtADFs (Dong et al., 2001a). Moreover, the regulated interaction of GFP-NtADF1, its S6A derivative, and its S6D derivative with actin cables observed in elongating pollen tubes (Figures 2 and 3) lends support to the nature of the association pattern observed for GFP-NtADF1 reported here.

The GFP-NtADF1–labeled actin mesh at the subapical pollen tube region (Figures 2 and 5) was observed even in pollen tubes that expressed the minimum detectable levels of the fusion protein. This finding suggests that NtADFs normally associate preferentially with actin filaments in the subapical actin mesh rather than in the long actin cables in the shank. At a higher, but not yet growth-inhibiting, level of GFP-NtADF1 expression (Figures 2 and 3), more actin cables and filaments along the shank of the pollen tubes were labeled with GFP-NtADF1.

However, pollen tube germination and growth apparently can tolerate only a certain level of ADF association with its organized actin cytoskeleton, because very high level expression of GFP-NtADF1 or GFP-NtADF1(S6A) resulted in highly bundled or patched actin (Figure 2A) and was deleterious to these processes. The stronger binding of GFP-NtADF1(S6A) to the actin cytoskeleton (Figures 2 and 3) and the pollen tube growth–inhibitory effect of NtADF1(S6A) (Figure 6B) relative to their wild-type counterparts are consistent with the idea that excessive binding of ADFs to organized actin structures is adverse to pollen tube growth. The relatively normal growth property in pollen tubes that overproduced the actin binding–incompetent NtADF1(S6D) (Figure 6B) also supports the idea that the level of ADF–actin interaction is more critical to this polar cell growth process than the absolute level of ADFs per se.

Anecdotally, transiently transformed pollen tubes provided the best samples for the imaging of the GFP-NtADF1 association with F-actin structures (Figures 2, 3, and 5) because of the tolerance of a broader range of transgene expression. Probably because of a strong tendency to regulate ADF to preserve the optimum pollen germination and tube growth ability, pollen from transformed plants produced relatively weaker GFP-NtADF1 expression. Their in vitro–grown pollen tubes did not permit such details to be discerned. On the other hand, the large amount of GFP-expressing pollen from stable transformed plants provided the opportunity to observe the ADF-labeled actin cytoskeleton in pollen tubes elongating within the pistil (Figure 7).

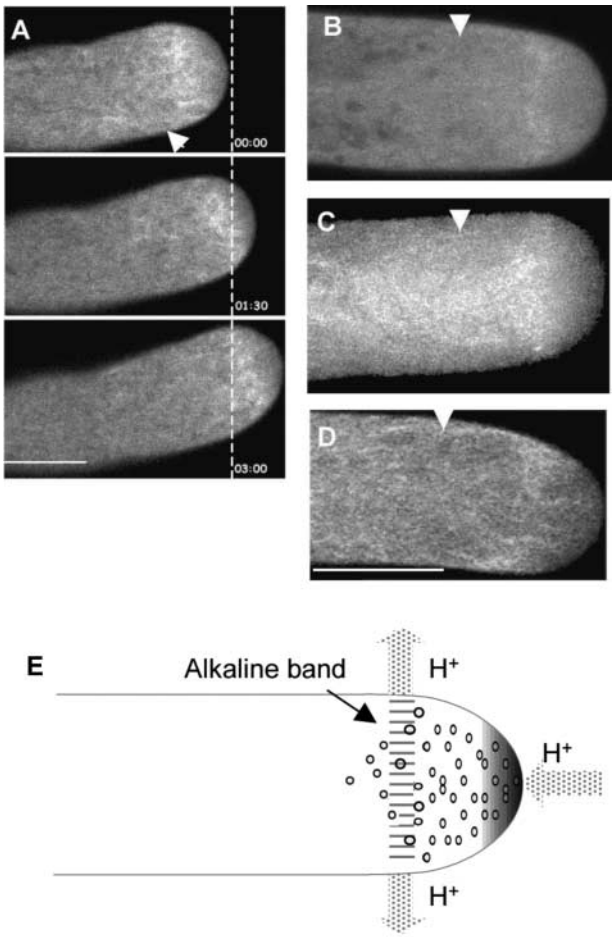

Figure 5. GFP-NtADF1 Is Concentrated in an Actin Mesh at the Subapical Region of Elongating Tobacco and Lily Pollen Tubes.

(A) Confocal images of a single optical section of the apical region of an elongating tobacco pollen tube expressing GFP-NtADF1 over a period of 180 s. Time interval is shown at lower right in each image. The dashed line indicates the location of the pollen tube tip at the beginning of this time series. Note that the orientation of the GFP-NtADF1–labeled mesh relative to the growth axis remained similar as the pollen tube growth trajectory changed over time. The dynamics within the GFP-NtADF1–labeled mesh can be observed best by viewing the supplemental data online.

(B) Confocal image of a single optical section of the apical region of an elongating lily pollen tube expressing GFP-LlADF1. See supplemental data online for a time sequence of this tube.

(C) A projection of optical images for an entire elongating lily pollen tube expressing GFP-LlADF1. The effect of growth is reflected by a relatively broad GFP-LlADF1–labeled mesh. The funnel-shaped structure trailing the subapical actin mesh reflects actin filaments that moved basipetally from the actin mesh.

(D) An elongating lily pollen tube showing a GFP-talin–labeled actin mesh at the subapical region. See supplemental data online for a time sequence of this tube.

(E) Scheme showing the distribution of H^+ fluxes (arrows) around a lily pollen tube tip region. A tip-focused H^+ gradient is shown, and increasing shading intensity indicates increasing concentration. An alkaline band (reported to be approximately pH 7.5, relative to a tip pH of 6.5) has been located within and close to the base of the clear zone (Feijo et al., 1999).

All pollen tubes shown in **(A)** to **(D)** were transformed transiently by microprojectile bombardment. Arrowheads at top in **(A)** to **(D)** point to the base of the clear zone as observed under differential interference contrast imaging. Small dots in **(E)** indicate secretory vesicles in the clear zone. Bar in **(A)** = 10 μm; bar in **(D)** = 20 μm for **(B)** to **(D)**.

Potential Functional Significance of the ADF-Rich Subapical Actin Mesh in Elongating Pollen Tubes

Latrunculin B (LatB) is a potent inhibitor of actin polymerization in different cell systems, including pollen (Gibbon et al., 1999). Maize pollen tube growth has been reported to be more sensitive to LatB than germination, leading to the speculation that tip growth depends on a small population of LatB-sensitive actin filaments (Gibbon et al., 1999). Consistent with this idea is the observation that LatB disrupts the subapical actin mesh in lily pollen tubes at a concentration substantially lower than that needed to disrupt the axially arranged long actin bundles in the shank (Vidali et al., 2001). Together, these observations support the view that the actin mesh at the base of the clear zone could be the site where active actin remodeling takes place to achieve the reversal in the cytoplasmic streams and where rapidly formed F-actin becomes incorporated into cables (Hepler et al., 2001; Vidali et al., 2001).

The presence of a pH gradient at the apical region of elongating pollen tubes (Feijo et al., 1999), the more efficient NtADF1 in vitro actin depolymerization activity at slightly alkaline pH (Figure 4B), the localization of an ADF-rich subapical actin mesh in elongating tobacco and lily pollen tubes (Figure 5), and the absence of this structure in growth-arrested pollen tubes strongly suggest a functional role for NtADFs in this subapical region. A subapical ADF-rich structure also was revealed in GFP-NtADF1–expressing pollen tubes elongating in pistil tissues (Figure 7E), extending the potential significance of this structure to the in vivo elongation process.

The stability of the orientation of this ADF-rich actin mesh relative to the growth axis in elongating tubes (Figure 5A) also suggests that it may be important in defining growth orientation. The actin-depolymerizing activity of NtADF1 at the subapical region of elongating pollen tubes most likely would be regulated spatially along the pH gradient (Feijo et al., 1999). It may be speculated that under slightly alkaline conditions, NtADF1 behaves like other pH-sensitive ADFs/cofilins, in that its F-actin–severing activity is favored. This would result in a higher number of fragmented filaments and generate more barbed ends for actin polymerization. This and enhanced minus-end actin-depolymerizing activity should significantly affect the dynamics of actin cycling in a region where actin filaments are expected to undergo rapid restructuring.

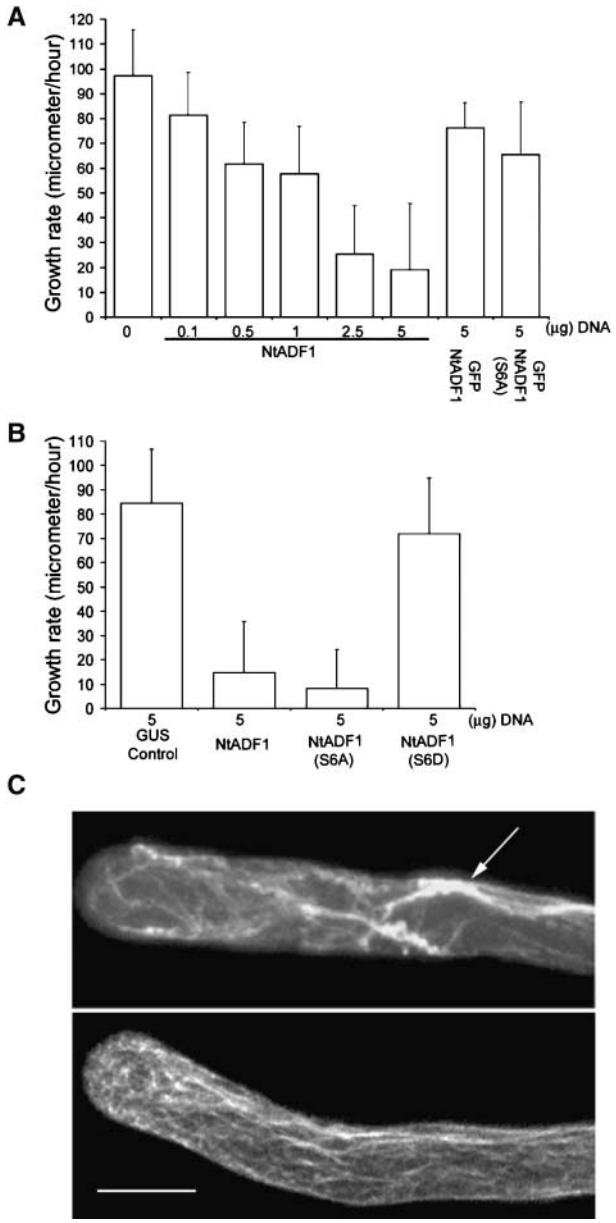

Figure 6. Overexpression of NtADF1 Inhibits Pollen Tube Growth in Transiently Transformed Pollen Tubes.

(A) and **(B)** Pollen tube growth rates between 5 and 8 h of growth after germination. Pollen was transformed with the indicated amounts of different chimeric genes used. In **(A)**, except for the GFP-NtADF1 and GFP-NtADF1(S6A) samples, all pollen grains were cobombarded with 5 μg of Lat52-GFP as a marker for transformation and to assess for comparable transgene expression in all samples. In samples in which <5 μg of experimental chimeric gene was used, Lat52–β-glucuronidase (GUS) DNA was added to make up to 10 μg of DNA used for every transformation. This ensured that equal amounts of DNA were coated onto tungsten particles and introduced into the pollen samples.

(C) Projection of Z-series images of 5-h-old pollen tubes that had been transformed with 5 μg of Lat52-GFP and 5 μg of Lat52-NtADF1 (top) or with the same amounts of Lat52-GFP and Lat52–β-glucuronidase (bottom; control), fixed, and stained with Texas red–conjugated phalloidin. Lat52-GFP served as a marker for transformation. The arrow points to thick phalloidin-bound actin bundles. Bar = 10 μm.

We are attempting to obtain a simultaneous localization of the ADF-rich actin mesh and the apical proton gradient in lily and tobacco pollen tubes. This, together with a detailed characterization of the pH sensitivity of the NtADF–actin interaction and its in vivo actin-depolymerizing activity, will be needed to formulate how ADF may be regulated spatially and how it contributes to actin remodeling by differential H^+ conditions in the pollen tube subapical region.

NtADF1 Is Important to Pollen Tube Growth

The inhibition of pollen tube growth rate by transiently overexpressed NtADF1, the more pronounced effect of overexpressing NtADF1(S6A), and the relatively ineffectiveness of overexpressing NtADF1(S6D) (Figure 6) suggest that the extent of NtADF1 interaction with actin is critical to this tip growth process. Relatively thin GFP-NtADF1–labeled actin cables usually were observed in transformed pollen tubes that elongated relatively normally in vitro (Figure 2). Previous studies have shown that pollen tube growth arrest was associated with actin disorganization at the subapical region and invasion of short actin bundles into the clear zone, whereas the cessation of cytoplasmic streaming was associated with disruption of the long axially arranged actin cables in the shank (Vidali et al., 2001).

The absence of the ADF-rich actin mesh in the subapical region of growth-arrested pollen tubes suggests a functional significance of this structure to growth. The disappearance of the thin, longitudinally arranged actin filaments in pollen tubes that overexpressed NtADF1 (Figure 6C) could be the basis of their growth-inhibitory activity. It is possible that the dynamics of the turnover of shank actin filaments needed to support a proper level and pattern of intracellular trafficking could not be maintained in the presence of excessive ADF binding to these long actin filaments. However, understanding the mechanism underlying the inhibitory effect of overexpressed NtADF1 on pollen tube growth will require more detailed knowledge of how its actin binding, severing, and enhanced minus-end depolymerizing activities are regulated in the pollen tube cytosol.

Plants transformed by *Lat52-GFP-NtADF1* and its S6A and S6D derivatives produced transformed pollen grains that, as a population, did not lead to appreciable differences in reproductive yields compared with controls. On the level of individual pollen grains, it was quite apparent that there

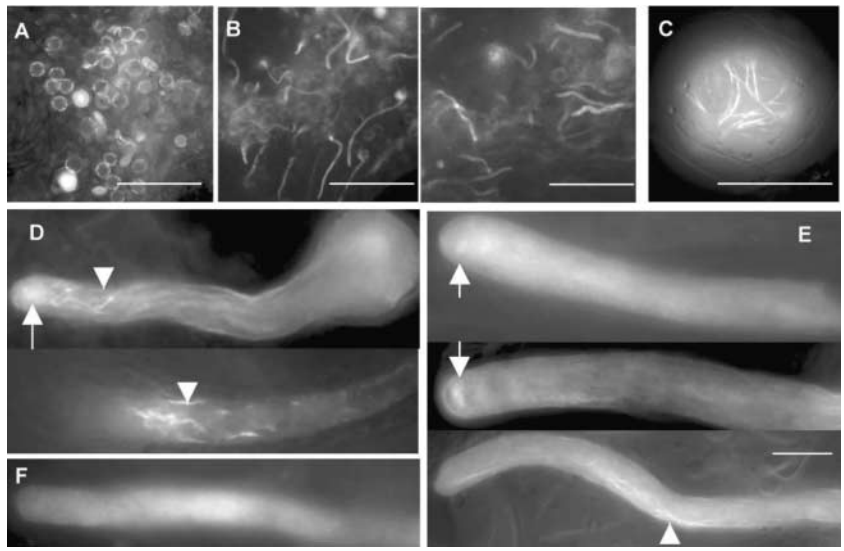

Figure 7. GFP-NtADF1 Localization Pattern in Transformed Pollen Tubes Elongating in the Pistil.

(A) Epifluorescence image of a representative stigma that had been pollinated with control GFP-expressing pollen grains. Only a few ungerminated grains remained, as occurs normally in all pollination. The nonfluorescent grains represent the empty grains whose cytoplasm had migrated with the pollen tube tip into the lower half of the style.
(B) Epifluorescence images of two representative stigmas that had been pollinated with GFP-NtADF1–expressing pollen grains. A larger number of short pollen tubes remained in the stigmatic regions relative to the control.
(C) Hydrated GFP-NtADF1–expressing pollen grain on the stigma.
(D) Two representative short GFP-NtADF1–expressing pollen tubes from the stigmatic region.
(E) Three representative GFP-NtADF1–expressing pollen tubes that had extended into the bottom half of pollinated styles.
(F) A control GFP-expressing pollen tube that had extended into the bottom half of a pollinated style showing only diffuse fluorescent signal.
Arrows point to the subapical region with a concentration of GFP-NtADF1. Arrowheads point to actin cables in the shank. Bars in **(A)** to **(C)** = 100 μm; bar in **(E)** = 10 μm for **(D)** to **(F)**.

was a low percentage of pollen grains that expressed levels of GFP-NtADF1 high enough to negatively affect germination competence and tube growth rates (Figure 7). This led us to suggest that endogenous mechanisms during pollen maturation might have exerted compensatory measures to ensure a level of expression and possible post-translational regulation of ADF activities so that pollen germination and tube growth may proceed.

It is interesting that in Arabidopsis, relatively mild morphological phenotypes were induced in transgenic plants that overproduced AtADF1 to 30 to 50 times the level of endogenous AtADFs. On the other hand, disruption of the normal actin cytoskeleton structure has been observed in a few specialized cell types (Dong et al., 2001b), suggesting that plant growth and developmental processes are more refractory to perturbation of this actin binding protein than cellular processes that associate with the actin cytoskeleton. Therefore, studies that rely on a transient transformation and expression system, such as those reported here, or on the application of regulated pollen expression in stable transformed plants will likely be the optimum combination to manipulate the activity of pollen actin cytoskeleton.

METHODS

Isolation of cDNAs

Mature pollen grains were collected from greenhouse-grown tobacco (*Nicotiana tabacum* cv Petit Havana SR1). Total RNA and poly(A)$^+$ RNA were isolated as described (Ausubel et al., 2000). Five micrograms of poly(A)$^+$ RNA was used for cDNA synthesis and library construction using the λZAPII-cDNA synthesis and library construct kits (Stratagene) according to the manufacturer's protocols.

AtADF1 cDNA (Carlier et al., 1997) was isolated by reverse transcriptase–mediated PCR of *Arabidopsis thaliana* leaf RNA and used as a probe to screen for tobacco actin-depolymerizing factor (*ADF*) cDNAs. Hybridization was performed in 0.5 M $NaHPO_4$, pH 7.2, 7% SDS, and 1 mM EDTA at 46°C overnight. The filters were washed three times for 20 min each in 2 × SSC (1× SSC is 0.15 M NaCl and 0.015 M sodium citrate) at 46°C. Positive plaques were purified by repeated screening. Phagemids were excised from pure phages, and several of the cDNA inserts were sequenced. LlADF from lily (*Lilium longiflorum*) anther ADF (Kim et al., 1993) was isolated by reverse transcriptase–mediated PCR from lily pollen RNA.

RNA Gel Blot Analysis

Total RNA was isolated from various tobacco organs. RNA gel blot analysis, transfer, and hybridization were performed according to previously described procedures (Kawata and Cheung, 1990).

Recombinant DNA Construction

Standard recombinant DNA methodology (Ausubel et al., 2000) was followed. A BamHI site was introduced by PCR to the 5′ end of NtADF1 and NtADF2 to create an in-frame fusion with the initiation codon of each of the clones. They were subcloned into the pBluescript KSII+ (Stratagene) vector and used for PCR-based mutagenesis (Ho et al., 1989; Ito et al., 1991). Wild-type and mutant cDNAs were fused in frame at a BglII site that had been introduced to the 3′ end of an engineered green fluorescent protein (GFP) cDNA (Chiu et al., 1996).

The fusion junction for the resultant chimeric genes had an insertion of two amino acid residues between GFP and the NtADF cDNAs. All fusion junctions were sequenced to confirm that in-frame fusion had been generated as designed. These fusion genes were cloned behind the pollen-specific promoter Lat52 (Twell et al., 1990) in the pBluescript SKII+ vector or were inserted into an intermediate vector for Ti plasmid transformation. The GFP-talin construct (Kost et al., 1999) was cloned behind the maize pZmc13 promoter (Hamilton et al., 1998) for expression in lily pollen tubes.

Microprojectile Bombardment

All plasmid DNA used was prepared by CsCl gradient purification. Undehisced anthers were collected from SR1 flowers and allowed to dehisce overnight. Ten milligrams of mature pollen grains was used in each bombardment. Pollen germination medium (0.01% H_3BO_3, 0.01% HNO_3, 0.02% $MgSO_4$, 0.07% $CaCl_2$, 15% PEG-3350, 2% Suc, and 20 mM Mes, pH 6) was used to culture pollen grains. Pollen suspension was spotted on 35-mm Petri dishes that contained germination medium without PEG-3350 and was solidified with 0.7% agarose.

Microprojectile bombardment was performed using the helium-driven PDS-1000/He biolistic system (Bio-Rad, Hercules, CA). Tungsten particles (1.1 μm) were coated with plasmid DNA according to the manufacturer's recommendation (Bio-Rad) (Sanford et al., 1993). Fifteen micrograms of DNA was used to coat 3 mg of tungsten particles, which were used in double bombardments of an individual pollen sample to increase the transformation frequency. The parameters of bombardment were as follows: 28-inch Hg chamber vacuum, 1100-psi rupture disc, 0.25-inch gap distance, and 1-inch particle travel distance. Cobombardment was achieved by coating particles with equal amounts of plasmid DNA, unless indicated otherwise.

In growth comparison experiments, Lat52 GFP was cobombarded as a marker for transformation and for the assessment of transgene expression level in each sample. In dose-dependent growth comparison experiments, samples also were cobombarded with different amounts of Lat52–β-glucuronidase, which was included to ensure that the same amount of DNA (10 μg) was coated onto the tungsten particles and delivered into pollen grains. Pollen tubes were observed directly on culture plates, recorded, and measured with the imaging software included in the camera package. On average, 25 tubes were counted for each sample.

Microscopic Observations

Fluorescence images were observed on a Nikon E800 microscope (Tokyo, Japan), recorded with a charge-coupled device camera (Spot, Diagnostic Instruments, Sterling Heights, MI), and edited with the image-processing software Photoshop 5.5 (Adobe Systems, Mountain View, CA). Confocal images were taken from a Bio-Rad 600 system equipped with argon and helium-neon lasers. GFP fluorescence images were collected using excitation with the 488-nm line of the argon laser (emission filter, 560-nm long pass; dichroic at 522 nm). The Texas red–conjugated phalloidin-staining pattern was imaged by 568-nm excitation generated by the helium-argon laser (emission, 560-nm long pass; dichroic at 605 nm). Time-series images were taken at 10-s intervals at one focal plane. Sequential images were edited into movies by GIF Animator (Ulead, Taipei, Taiwan). Z-series images were collected at 1-μm steps and projected by Confocal Assistant imaging software (Bio-Rad). Artificial colors were applied to some raw images using Photoshop 5.5. Merged images were created by overlaying two images and were edited with contrast enhancement.

Phalloidin Staining

Transformed pollen tubes were immobilized by 0.7% low-melting agarose on cover slips 3 h after bombardment. After plating, pollen tubes were allowed to recover in a moisture chamber with germination medium for 1 h. Chemical fixation procedures (Doris and Steer, 1996; Vidali et al., 2001) were applied to preserve pollen tubes. First, pollen tubes were treated with 300 μM *m*-maleimidobenzoyl-*N*-hydroxysuccinimide ester and 271 μM disuccinimidyl suberate (Pierce) in germination medium for 15 min. Freshly prepared 2% paraformaldehye in 70 mM KCl, 1 mM $MgCl_2$, 1 mM $CaCl_2$, and 0.1 M Pipes, pH 6.5 (MKCP buffer), was used to fix pollen tubes for 30 min. Fixed pollen tubes then were incubated in Texas red–conjugated phalloidin (Molecular Probes, Eugene, OR) with permeabilization buffer (0.1% Triton X-100 and MKCP buffer) for 30 to 60 min. Excess phalloidin was removed by permeabilization buffer with 1 mM DTT.

In Vitro NtADF1 and Actin Interaction

Muscle actin was purified from the acetone powder of chicken breast according to Pardee and Spudich (1982), followed by a gel filtration step on Sephadex G-150 (MacLean-Fletcher and Pollard, 1980). Purified actin was frozen rapidly in liquid N_2 and stored at −80°C until needed. The coding regions of wild-type and mutant NtADF1 were cloned into pET-15b vector (Novagen, Madison, WI). His6-tagged NtADF1s were expressed in *Escherichia coli* BL21(DE3) and purified with a Talon affinity column (Clontech, Palo Alto, CA) according to the manufacturer's protocol.

The His6 tag was cleaved from the fusion proteins by thrombin digestion. Thrombin was removed with *p*-aminobenzamidine agarose beads (Sigma). Purified proteins were dialyzed against 10 mM Tris-HCl, pH 8.0, 50 mM KCl, and 1 mM DTT or 10 mM Hepes, pH 7.0, 50 mM KCl, and 1 mM DTT, depending on the experiments that followed. Protein concentrations were determined spectrophotometrically using extinction coefficients of $0.617 mg^{-1} \cdot cm^2$ for actin at 290 nm and $0.89\ mg^{-1} \cdot cm^2$ for NtADF1s at 278 nm (Carlier et al., 1997) and were confirmed by SDS-PAGE.

F-Actin Sedimentation

Purified actin was polymerized in buffer A (2 mM Tris-HCl, pH 8, 0.2 mM ATP, 0.5 mM β-mercaptoethanol, 0.2 mM $CaCl_2$, and 0.005% azide) with 1 × KME (50 mM KCl, 1 mM $MgCl_2$, 1 mM ATP, and 1 mM EGTA) on ice for 1 h. Twelve micromolar F-actin was mixed with different amounts of NtADF1 protein, and the total volume was adjusted to 100 μL with 1 × KME and 50 mM Tris-HCl, pH 8.0, or 50 mM Mes, pH 6.

The reactions were incubated on ice for 1 h and centrifuged using a 42.2 Ti rotor (Beckman) for 45 min at 28,000 rpm and 4°C. Supernatants were collected after centrifugation, and the pellets were resuspended in the original volume of SDS-PAGE loading buffer. The same volume of samples from supernatants and pellets was loaded for SDS-PAGE, and proteins were detected by Coomassie Brilliant Blue R250 staining.

Upon request, all novel materials described in this article will be made available in a timely manner for noncommercial research purposes. No restrictions or conditions will be placed on the use of any materials described in this article that would limit their use for noncommercial research purposes.

Accession Numbers

The GenBank accession numbers for the sequences mentioned in this article are AY081941 (NtADF1), AY081942 (NtADF2), Q39250 (Arabidopsis AtADF1), P46251 (maize pollen ZmADF1), Q41764 (constitutive ZmADF3), Q03048 (yeast cofilin), NP_006861 (human dextrin), and CAA78483 (lily anther LlADF).

ACKNOWLEDGMENTS

We thank Dany Adam and Richard Briggs of Smith College for the generosity of their time and confocal facility. We thank Sheila McCormick for the Lat52 promoter, which we modified for easier cloning purposes, N.-H. Chua for a clone of the Lat52-GFP-talin, and J. Mascarenhas for a clone of the pZmc13 promoter. We thank Maura Cannon for the use of her Biolistic Microprojectile Bombardment equipment. We thank an anonymous reviewer for many thoughtful comments scientifically and for improving the presentation of our data. Confocal microscopy was performed at the University of Massachusetts Central Microscopic Facility, which is supported partially by Grant BBS8714235 from the National Science Foundation. This work was supported by grants from the National Institutes of Health (GM52953) and the Department of Energy (97ER20288).

Received March 13, 2002; accepted June 4, 2002.

REFERENCES

Agnew, B.J., Minamide, L.S., and Bamburg, J.R. (1995). Reactivation of phosphorylated actin depolymerizing factor and identification of the regulatory site. J. Biol. Chem. **270,** 17582–17587.

Aizawa, H., Fukui, Y., and Yahara, I. (1997). Live dynamics of *Dictyostelium* cofilin suggests a role in remodeling actin latticework into bundles. J. Cell Sci. **110,** 2333–2344.

Aizawa, H., Suton, K., and Yahara, I. (1996). Overexpression of cofilin stimulates bundling of actin filaments, membrane ruffling, and cell movement in *Dictyostelium*. J. Cell Biol. **132,** 335–344.

Ausubel, F.M., Brent, R., Kingston, R.E., Moore, D.D., Seidman, J.G., Smith, J.A., and Struhl, K. (2000). Current Protocols in Molecular Biology. (New York: John Wiley & Sons).

Bamburg, J.R. (1999). Proteins of the ADF/cofilin family: Essential regulators of actin dynamics. Annu. Rev. Cell Biol. **15,** 185–230.

Bamburg, J.R., McGough, A., and Ono, S. (1999). Putting a new twist on actin: ADF/cofilins modulate actin dynamics. Trends Cell Biol. **9,** 364–370.

Bernstein, B.W., Painter, W.B., Chen, H., Minamide, L.S., Abe, H., and Bamburg, J.R. (2000). Intracellular pH modulation of ADF/cofilin proteins. Cell Motil. Cytoskeleton **47,** 319–336.

Bowman, G.D., Nodelman, I.M., Hong, Y., Chua, N.-H., Lindberg, U., and Schutt, C.E. (2000). A comparative structural analysis of the ADF/cofilin family. Proteins Struct. Funct. Genet. **41,** 374–384.

Carlier, M.-F. (1998). Control of actin dynamics. Curr. Opin. Cell Biol. **10,** 45–51.

Carlier, M.-F., Laurent, V., Santolini, J., Melki, R., Didry, D., Xia, G.-X., Hong, Y., Chua, N.-H., and Pantaloni, D. (1997). Actin depolymerizing factor (ADF/cofilin) enhances the rate of filament turnover: Implication in actin-based motility. J. Cell Biol. **136,** 1307–1323.

Chen, C.Y. (2002). Functional Analysis of Actin Depolymerizing Factors in Rac-Mediated Pollen Tube Growth. PhD dissertation (Amherst: University of Massachusetts).

Cheung, A.Y., Chen, C., Glaven, R.H., De Graaf, B., Vidali, L., Hepler, P., and Wu, H.-M. (2002). Rab2 GTPase regulates membrane trafficking between endoplasmic reticulum and Golgi and is important to pollen tube growth. Plant Cell **14,** 945–962.

Cheung, A.Y., and Wu, H.-M. (2001). Pollen tube guidance: Right on target. Science **293,** 1441–1442.

Chiu, W., Niwa, Y., Zeng, W., Hirano, T., Kobayashi, H., and Sheen, J. (1996). Engineered GFP as a vital reporter in plants. Curr. Biol. **6,** 325–330.

Derksen, J., Rutten, T., Van Amstel, T., de Win, A., Doris, F., and Steer, M. (1995). Regulation of pollen tube growth. Acta Bot. Neerl. **44,** 93–119.

Dong, C.H., Kost, B., Xia, G., and Chua, N.H. (2001a). Molecular identification and characterization of the *Arabidopsis* AtADF1, AtADF5 and AtADF6 genes. Plant Mol. Biol. **45,** 517–527.

Dong, C.H., Xia, G.X., Hong, Y., Ramachandran, S., Kost, B., and Chua, N.H. (2001b). ADF proteins are involved in the control of flowering and regulate F-actin organization, cell expansion, and organ growth in Arabidopsis. Plant Cell **13,** 1333–1346.

Doris, F.P., and Steer, M.W. (1996). Effects of fixatives and permeabilization buffers on pollen tubes: Implications for localization of actin microfilaments using phalloidin staining. Protoplasma **195,** 25–36.

Federov, A.A., Lappalainen, P., Federov, E.V., Drubin, D.G., and Almo, S.C. (1997). Structure determination of yeast cofilin. Nat. Struct. Biol. **4,** 366–369.

Feijo, J.A., Sainhas, J., Hackett, G.R., Kunkel, J.G., and Hepler, P. (1999). Growing pollen tubes possess a constitutive alkaline

band in the clear zone and a growth-dependent acidic tip. J. Cell Biol. **144,** 483–496.

Franklin-Tong, V.E. (1999). Signaling in pollination. Curr. Opin. Plant Biol. **2,** 490–495.

Fu, Y., Wu, G., and Yang, Z. (2001). Rop GTPase-dependent dynamics of tip-localized F-actin controls tip growth in pollen tubes. J. Cell Biol. **152,** 1019–1032.

Geitmann, A., Snowman, B.N., Emons, A.M., and Franklin-Tong, V.E. (2000). Alterations in the actin cytoskeleton of pollen tubes are induced by the self-incompatibility reaction in *Papaver rhoeas*. Plant Cell **12,** 1239–1251.

Gibbon, B.C., Dovar, R.K., and Staiger, C.J. (1999). Latrunculin B has different effects on pollen germination and tube growth. Plant Cell **11,** 2349–2363.

Gungabissoon, R.A., Jiang, C.-J., Drobak, B.K., Maciver, S.K., and Hussey, P.J. (1998). Interaction of maize actin-depolymerizing factor with actin and phosphoinositides and its inhibition of plant phospholipase C. Plant J. **16,** 689–696.

Hamilton, D.A., Schwarz, Y.H., and Mascarenhas, J.P. (1998). A monocot pollen-specific promoter contains separable pollen-specific and quantitative elements. Plant Mol. Biol. **38,** 663–669.

Hawkins, M., Pope, B., Maciver, S.K., and Weeds, D.G. (1993). Human actin depolymerizing factor mediates a pH-sensitive destruction of actin filaments. Biochemistry **32,** 9985–9993.

Hayden, S.M., Miller, P.S., Brauweiler, A., and Bamburg, J.R. (1993). Analysis of the interactions of actin depolymerizing factor with G- and F-actin. Biochemistry **32,** 9994–10004.

Hepler, P.K., Vidali, L., and Cheung, A.Y. (2001). Polarized cell growth in higher plants. Annu. Rev. Cell Dev. Biol. **17,** 159–187.

Ho, S.N., Hunt, H.D., Horton, R.M., Pullen, J.K., and Pease, L.R. (1989). Site-directed mutagenesis by overlap extension using the polymerase chain reaction. Gene **77,** 51–59.

Huang, S., McDowell, J.M., Weise, M.J., and Meagher, R.B. (1996). The *Arabidopsis* profilin gene family: Evidence for an ancient split between constitutive and pollen-specific profilin genes. Plant Physiol. **111,** 115–126.

Iida, K., and Yahara, J. (1999). Cooperation of two actin binding proteins, cofilin and Aip1, in *Saccharomyces cerevisiae*. Genes Cells **4,** 21–32.

Ito, W., Ishiguro, H., and Kurosawa, F. (1991). A general method for introducing a series of mutations into cloned DNA using the polymerase chain reaction. Gene **102,** 67–70.

Jiang, C.J., Weeds, A.G., and Hussey, P.J. (1997a). The maize actin-depolymerizing factor, ZmADF3, redistributes to the growing tip of elongating root hairs and can be induced to translocate into the nucleus with actin. Plant J. **12,** 1035–1043.

Jiang, C.J., Weeds, A.G., Khan, S., and Hussey, P.J. (1997b). F-actin and G-actin binding are uncoupled by mutation of conserved tyrosine residues in maize actin depolymerizing factor (ZmADF). Proc. Natl. Acad. Sci. USA **94,** 9973–9978.

Kawata, E.E., and Cheung, A.Y. (1990). Molecular analysis of an aurea photosynthetic mutant (Su/Su) in tobacco: LHCP depletion leads to pleiotropic mutant phenotypes. EMBO J. **9,** 4197–4203.

Kim, S.R., Kim, R., and An, G. (1993). Molecular cloning and characterization of anther-preferential cDNA encoding a putative actin-depolymerizing factor. Plant Mol. Biol. **21,** 39–45.

Kost, B., Lemichez, E., Spielhofer, P., Hong, Y., Tolias, K., Carpenter, C., and Chua, N.H. (1999). Rac homologues and compartmentalized phosphatidylinositol 4,5-bisphosphate act in a common pathway to regulate polar pollen tube growth. J. Cell Biol. **145,** 317–330.

Lappalainen, P., and Drubin, D.G. (1997). Cofilin promotes rapid actin filament turnover *in vivo*. Nature **388,** 78–82.

Lappalainen, P., Federov, E., Federov, A.A., Almo, S.C., and Drubin, D.G. (1997). Essential functions and actin-binding surfaces of yeast cofilin revealed by systematic mutagenesis. EMBO J. **18,** 5520–5530.

Leonard, S.A., Gittis, A.G., Petrella, E.C., Pollard, T.D., and Lattman, E.E. (1997). Crystal structure of the actin-binding protein actophorin from *Acanthamoeba*. Nat. Struct. Biol. **4,** 369–373.

Lopez, I., Anthony, R.G., Maciver, S.K., Jiang, C.J., Khan, S., Weeds, A.G., and Hussey, P.J. (1996). Pollen specific expression of maize genes encoding actin depolymerizing factor-like proteins. Proc. Natl. Acad. Sci. USA **93,** 7415–7420.

Lord, E. (2000). Adhesion and cell movement during pollination: Cherchez la femme. Trends Plant Sci. **5,** 368–373.

Maciver, S.K. (1998). How ADF/cofilin depolymerizes actin filaments. Curr. Opin. Cell Biol. **10,** 140–144.

Maciver, S.K., Pope, B.J., Whytock, S., and Weeds, A.G. (1998). The effect of two actin depolymerizing factors (ADF/cofilins) on actin filament turnover: pH sensitivity of F-actin binding by human ADF, but not of *Acanthamoeba* actophorin. Eur. J. Biochem. **256,** 388–397.

Maciver, S.K., Zot, H.G., and Pollard, T.D. (1991). Characterization of actin filament severing by actophorin from *Acanthamoeba castellanii*. J. Cell Biol. **115,** 1611–1620.

MacLean-Fletcher, S., and Pollard, T. (1980). Identification of a factor in conventional muscle actin preparations which inhibits actin filament self-association. Biochim. Biophys. Res. Commun. **96,** 18–27.

McCurdy, D.W., Kovar, D.R., and Staiger, C.J. (2001). Actin and actin-binding proteins in higher plants. Protoplasma **215,** 89–104.

McGough, A., and Chiu, W. (1999). ADF/cofilin weakens lateral contacts in the actin filament. J. Mol. Biol. **291,** 513–519.

McGough, A., Pope, B., Chiu, W., and Weeds, A.G. (1997). Cofilin changes the twist of F-actin: Implications for actin filament dynamics and cellular function. J. Cell Biol. **138,** 771–781.

Meagher, R.B., McKinney, E.C., and Kandasamy, M.K. (1999a). Isovariant dynamics expand and buffer the responses of complex systems: The diverse plant actin gene family. Plant Cell **11,** 995–1005.

Meagher, R.B., McKinney, E.C., and Vitale, A.V. (1999b). The evolution of new structures: Clues from plant cytoskeletal genes. Trends Genet. **15,** 278–284.

Meberg, P.J., and Bamburg, J.R. (2000). Increase in neurite outgrowth mediated by overexpression of actin depolymerizing factor. J. Neurosci. **20,** 2459–2469.

Moriyama, K., Iida, K., and Yahara, I. (1996). Phosphorylation of ser-3 of cofilin regulates its essential function on actin. Genes Cells **1,** 73–86.

Palanivelu, R., and Preuss, D. (2000). Pollen tube targeting and axon guidance: Parallels in tip growth mechanisms. Trends Cell Biol. **10,** 517–524.

Pantaloni, D., Le Clainche, C., and Carlier, M.-F. (2001). Mechanism of actin-based motility. Science **292,** 1502–1506.

Pardee, J., and Spudich, J. (1982). Purification of muscle actin. Methods Enzymol. **85,** 164–211.

Pollard, T.D., Blanchoin, L., and Mullins, R.D. (2000). Molecular mechanisms controlling actin filament dynamics in nonmuscle cells. Annu. Rev. Biophys. Biomol. Struct. **29,** 545–576.

Sanford, J.C., Smith, F.D., and Russell, J.A. (1993). Optimizing the biolistic process for different biological applications. Methods Enzymol. **217,** 483–509.

Smertenko, A.P., Allwood, E.G., Khan, S., Jiang, C.J., Macier, S.K., Weeds, A.G., and Hussey, P.J. (2001). Interaction of pollen-specific actin-depolymerizing factor with actin. Plant J. **25,** 203–212.

Smertenko, A.P., Jiang, C.-J., Simmons, N.J., Weeds, A.G., Davies, D.R., and Hussey, P.J. (1998). Ser6 in the maize actin-depolymerizing factor, ZmADF3, is phosphorylated by a calcium-stimulated protein kinase and is essential for control of functional activity. Plant J. **14,** 187–193.

Staiger, C.J. (2000). Signaling to the actin cytoskeleton in plants. Annu. Rev. Plant Physiol. Plant Mol. Biol. **51,** 257–288.

Staiger, C.J., Gibbon, B.C., Kovar, D.R., and Zonia, L.E. (1997). Profilin and actin depolymerizing factor: Modulators of actin organization in plants. Trends Plant Sci. **2,** 275–281.

Steer, M.W., and Steer, J.M. (1989). Pollen tube tip growth. New Phytol. **111,** 323–358.

Theriot, J.A. (1997). Accelerating on a treadmill: ADF/cofilin promotes rapid actin filament turnover in the dynamic cytoskeleton. J. Cell Biol. **136,** 1165–1168.

Tsien, R.Y. (1998). The green fluorescent protein. Annu. Rev. Biochem. **67,** 509–544.

Twell, D., Yamaguchi, J., and McCormick, S. (1990). Pollen-specific gene expression of two different tomato gene promoters during microsporogenesis. Development **109,** 705–713.

Vidali, L., and Hepler, P.K. (1997). Characterization and localization of profilin in pollen grains and tubes of *Lilium longiflorum*. Cell Motil. Cytoskeleton **36,** 323–328.

Vidali, L., and Hepler, P.K. (2001). Actin and pollen tube growth. Protoplasma **215,** 64–67.

Vidali, L., McKenna, S.T., and Hepler, P.K. (2001). Actin polymerization is essential for pollen tube growth. Mol. Biol. Cell **12,** 2534–2545.